

Analysis of Thin Bifacial Silicon Solar Cells with Locally Diffused and Selective Back Surface Field

Adriano Moehlecke*, Vanessa da Conceição Osório, Izete Zanesco

Solar Energy Technology Nucleus, Faculty of Physics, Pontifical Catholic University of Rio Grande do Sul – PUCRS, Av. Ipiranga, 6681, P. 96A, TECNOPUC, CEP 90619-900, Porto Alegre, RS, Brazil

Received: May 6, 2014; Accepted: August 2, 2014

The aim of this work is to present the development and comparison of thin n⁺pp⁺ industrial bifacial silicon solar cells produced with the local screen-printed Al back surface field (BSF) to those with the selective BSF doped with aluminum-boron. To produce solar cells with selective BSF, the boron diffusion based on spin-on dopant was introduced in the process sequence. The thin SiO₂ layer (10 nm) thermally grown did not produce good passivation on the rear face and wafers were contaminated during aluminum diffusion in the belt furnace. The implementation of selectively doped BSF improved the efficiency by reflecting minority charge carriers and the wafer contamination by belt furnace was compensated by boron diffusion. The bifacial solar cells with B-Al selective BSF achieved an efficiency of 13.7% / 8.9% (front / rear illumination) and presented lower sensitivity to the belt furnace processing and to the quality of the rear surface passivation.

Keywords: *thin solar cells, bifacial solar cells, locally diffused Al-BSF, selective BSF*

1. Introduction

In the last decade, significant cost reductions in the kWh obtained from photovoltaic modules were related to the “economy-of-scale” benefits, the solar cell efficiency increase and the lower consumption of high purity silicon per Wp. For instance, wafer thickness was reduced from 350 μm to 180 μm. However, the silicon wafer still represents 58% of the cell cost and 42% of the PV module production costs¹. The use of thinner wafers can lead to cost reduction, but high quality surface passivation is needed to achieve high efficiency devices². Under the point of view of industrial processing, equipments need to be adapted for handling thin wafers³ and the standard n⁺pp⁺ silicon solar cells, with the rear surface fully covered by the Al thick layer, have to be modified in order to avoid the wafer bowing^{4,5}. The Al layer forms a back surface field that reflects the minority charge carriers away from the rear contact, reducing the recombination. The bow is produced during the thermal step performed to diffuse Al into a silicon wafer and it is a result of the different thermal coefficients of expansion of aluminum layer and silicon. The wafer bowing can lead to cracking during soldering and lamination processes used to assemble the PV modules.

In order to avoid the wafer bowing, solar cells with a rear metal grid and surface passivation based on dielectric films have been studied. For instance, Lee et al.⁶ produced large area PERC (passivated emitter rear cell) solar cells and achieved the efficiency of 17.7% by using 148.6 cm² FZ (float-zone) Si wafers and the efficiency of 17.2% in 156.8 cm² multicrystalline Si wafers. The wafers used had a thickness of 130 μm and the rear side was passivated with the SiO_x/SiN_x/SiO_xN_y stack deposited by PECVD

(plasma-enhanced chemical vapor deposition) and also by implementing the local back contacts using a laser. Front emitter was doped with phosphorus diffused in a quartz tube furnace by using POCl₃ as source. With the same goal of reducing bowing, Gu et al.⁵ implemented a BSF (back surface field) region by using a thin layer composed by boron and aluminum pastes deposited by screen-printing. The authors reported that the metallization paste thickness was reduced while the efficiency was not diminished. Therefore, thinner layer of doping paste fired at temperatures up to 800 °C can help the development of low bowing silicon solar cells.

Bifacial cells have been studied since the 1960s years⁷. This kind of cell is active in both faces and can convert the radiation reflected by the surrounding areas⁸. The bifacial cells also can be applied in static concentrators with different designs^{9,10,11}. Several bifacial structures were developed by using silicon as starting material^{7,12}. Simplified bifacial cells are based on the standard monofacial structure with one pn junction, one BSF region and the metal grid on both faces. This way, the use of a metal grid on the rear face avoids the bow and thinner wafers can be used. To obtain high electric current when the solar cell is illuminated by BSF region, the minority charge carrier diffusion length needs to be larger than the wafer thickness. Thus, the carriers photogenerated far from pn junction could be collected. Taking into account similar front and rear passivation, minority carrier diffusion length has to be over twice the wafer thickness to allow the production of symmetric bifacial cells, that is, cells with similar short-circuit electric current for front and rear side illumination^{13,14}.

High efficiency bifacial cells based on n⁺pp⁺ structure and using standard 200 μm thick Cz-grown (Czochralski)

*e-mail: moehlecke@pucrs.br

silicon wafers were reported by Yang et al.¹⁵. Homogeneous n^+ and p^+ regions were obtained by P and B diffusion performed at 870 °C and 1020 °C, respectively. $POCl_3$ and BBr_3 liquid sources were used in the diffusion processes. SiN_x antireflection/passivation coating was deposited on both faces as well as the screen printed metal grid. The large area devices (149 cm²) achieved the front and rear efficiencies of 16.6% and 12.8%, respectively. Janben et al.¹⁶ also used p-type Cz-Si and screen-printed contacts, but instead to implement a uniform p^+ region on the rear face, an Al metal grid was deposited to produce a local BSF. Front and rear surfaces were covered with an a- $SiN_x:H$ layer deposited by PECVD. The front and rear efficiency of 17% and 10.3%, respectively, were reported¹⁵.

Standard p^+nn^+ structure with homogenous doped regions was applied to produce small (4 cm²) FZ and Cz-silicon solar cells, achieving efficiencies of 19.1% / 18.1% (front / rear illumination) and 17.7% / 15.2%, respectively. The wafers employed were 250 μ m thick and the metal grid was defined by photolithography and deposited by e-beam evaporation at high vacuum^{17,18}. Buck et al.¹⁹ obtained efficiencies of 15.9% / 13.4% (front/rear illumination) in large area (144 cm²) p^+nn^+ devices fabricated by using FZ silicon wafer (200 mm thick) and with metal grid deposited by screen-printing. They also used BBr_3 and $POCl_3$ as diffusion sources to form p^+ and n^+ homogeneously doped regions.

The thin silicon bifacial cells have been developed by implementing n^+pp^+ , p^+nn^+ or n^+p structures. In small area devices (4 cm²) with evaporated contacts, front and rear efficiencies of 17% / 14.9% and 16% / 13% were reported for p^+nn^+ and n^+pp^+ cells, respectively²⁰. Homogenous n^+ and p^+ regions were obtained by P and B diffusion in 140 μ m thick Cz wafers. Using screen printed emitter and BSF as well as evaporated contacts, Pérez et al.²¹ reported small area bifacial devices that achieved the efficiencies of 14.2% / 13.6%. When screen-printed metal grids were implemented, efficiencies were lower: 11.6% / 10.8% for n^+pp^+ cells and 8.3% / 8.0% for p^+nn^+ ones. Bifacial n^+np^+ cells with a thickness of 130 μ m were developed by using a fully industrial in-line process²². The n^+ and p^+ regions were implemented by screen-printing deposition of phosphorus and boron pastes and the dopants were co-diffused into silicon wafers in the belt furnace. Metal grids were also deposited by screen-printing. Small area (4 cm²) devices achieved the front/rear efficiency of 13.6% / 10.4%²². Recart²³ developed larger bifacial devices (24.7 cm²) in 120 μ m thick Cz wafers by using screen-printed boron pastes to obtain p^+ BSF, but n^+ emitter was formed by phosphorus diffusion utilizing $POCl_3$ as source. The n^+pp^+ solar cells reached the efficiencies of 14.3% and 10.8% for front and rear side illumination, respectively. Thin bifacial cells with n^+ front emitter and the rear surface passivated with a SiN_x layer was presented by Steckemetz et al.²⁴. The SiN_x layer produced an effective passivation on the rear face and 14.6% / 13.6% (front/rear illumination) efficient devices were reported. Wafer thickness was 140 μ m and devices had the area of 4 cm².

The aim of this paper is to present the development and comparison of thin n^+pp^+ bifacial cells produced by using

the locally aluminum doped back surface field and by using the selective region doped with aluminum and boron. The process to obtain the selective p^+ region was based on boron deposition by spin-on and diffusion in the standard quartz tube followed by Al grid screen-printing and diffusion in a belt furnace. As far as we know, the combination of both processes to accomplish the selective BSF was used for the first time to produce thin bifacial solar cells. The devices were fabricated on solar grade Cz silicon wafers with the thickness of around 150 μ m by using industrial techniques. Surface passivation of a SiO_2 thin layer was also analyzed.

2. Material and Methods

The starting material was Cz-silicon, p-type, boron doped, 1-20 Ω .cm, <100> orientation. The thickness of the wafers was of around 150 μ m. The saw damage of the wafers was removed by immersing them in a KOH solution and the etching time defined the thickness of the wafers. Texture etch was carried out in an alkaline solution also based on KOH, but with lower concentration.

To develop the n^+pp^+ solar cells with locally diffused Al BSF, the process sequence shown in Figure 1a was used. Wafers were cleaned in RCA standard solutions and a 100 nm thick SiO_2 layer was grown at 1000 °C in a quartz tube furnace. Photoresist was spin coated on one face and the oxide layer was etched away in a buffered HF solution. After cleaning the wafers, the phosphorus diffusion was accomplished in a quartz tube furnace at 875 °C with $POCl_3$ as source. Phosphorus profile was measured by ECV (electrochemical capacitance-voltage) technique. The diffusion processes formed the n^+ emitter with a sheet resistance of 32 Ω/\square , with a junction depth of around 0.6 mm and surface concentration (C_s) of approximately 3.3×10^{19} cm⁻³. Phosphorus silicate glass (PSG) and SiO_2 layer were removed in an HF bath and wafers were cleaned in RCA solutions. A 10 nm thick SiO_2 layer was grown at 800 °C in order to passivate the surfaces. Cells without oxide were also processed to evaluate the passivation effectiveness of the SiO_2 layer. The titanium dioxide antireflection coating (ARC) was deposited by e-beam evaporation at high vacuum on the front face and the metal grid was deposited by screen-printing on both faces. In the first batches, ARC was not deposited on the rear face in order to avoid the misleading effects related to the TiO_2 etching process performed during the firing of Al paste. The silver paste was deposited on the front face and the Al paste was screen-printed on the rear face. The metal pastes were dry and co-fired in a belt furnace. The diffusion/firing temperature (T_{Firing}) used for cells without oxide layer was 840 °C and for those with a 10 nm thick SiO_2 layer was 850 °C²⁵. The metal grid was a standard H-pattern with two busbars, covering 9.5% of the surfaces (front and rear). Pseudo-square cells (80 mm \times 80 mm) were obtained after performing the edge isolation step.

The n^+pp^+ cells with selective BSF region doped with boron and Al were processed as summarized in Figure 1b. After the texture etch and the RCA cleaning, p^+ region was obtained by boron spin-on deposition and diffusion in a quartz tube furnace at 1000 °C. Boron diffusion was performed before phosphorus in order to avoid the production of a very deep pn junction and thicker dead layer,

which occurs when phosphorus is diffused in supersaturation conditions. The oxide layer needed to mask the p⁺ region from the phosphorus diffusion was grown in the same thermal step of the boron diffusion. Photoresist was spin coated on the boron-doped face and the oxide layer was etched away in a buffered HF solution. Phosphorus was diffused at 875 °C (POCl₃ as source). Phosphorus and boron silicate glasses (PSG and BSG) were etched away by means of HF solution and RCA cleaning was performed. Silicon dioxide layer was grown and TiO₂ ARC was deposited. Ag and Al metal grids were screen-printed on the front and rear face, respectively, and were co-fired in the belt furnace. The diffusion/firing temperatures were the same used for cells with local Al-BSF. Boron diffusion resulted in the doped region with a thickness of around 1 μm, surface concentration of 3.6 × 10¹⁹ cm⁻³ and sheet resistance of 30 Ω/□. The n⁺ emitter presented the sheet resistance of approximately 32 Ω/□.

All the devices were characterized under standard conditions (100 mW/cm², AM1.5G and 25 °C) in a solar simulator calibrated with silicon solar cells previously measured at CalLab - FhG-ISE (*Fraunhofer-Institut für Solare Energiesysteme*), Germany. Two-dimensional

distribution of minority charge carrier lifetime (τ) was obtained by μ -PCD (microwave photoconductivity decay) with the WT1000-PV device of Semilab. Minority charge carrier diffusion length (L_D) was calculated from LBIC (light beam induced current) measurements performed with the WT1000-PV equipment.

3. Results and Discussion

Table 1 presents the open circuit voltage (V_{oc}), the short-circuit current density (J_{sc}), the fill factor (FF), the efficiency (η) and the current symmetry factor (CSF) of the bifacial solar cells with local Al-BSF. The average values were calculated from the results of at least three cells. Quality of bifacial cells can be evaluated by the current symmetry factor CSF (also called “bifaciality”) defined as the ratio of the short-circuit current when the cell is illuminated on the rear face to the one when the cell is illuminated on the front face.

The solar cells with SiO₂ passivated surfaces presented an average V_{oc} of 9-10 mV higher than that from unpassivated ones. The short-circuit current was increased by implementing SiO₂ film when the cell was illuminated

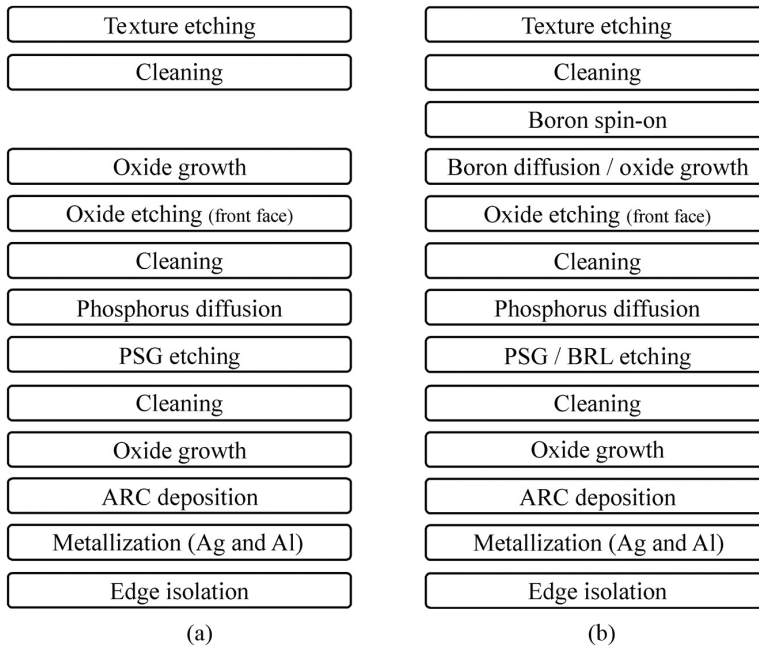


Figure 1. Bifacial solar cell process sequences: (a) devices with local Al-BSF and (b) with selective BSF (Al and B).

Table 1. Average electrical characteristics of bifacial solar cells with Al locally diffused BSF.

Front illumination (on n ⁺ p junction)					
	T _{Firing} (°C)	V _{oc} (mV)	J _{sc} (mA/cm ²)	FF	η (%)
Without SiO ₂	840	572 ± 3	29.7 ± 0.6	0.69 ± 0.02	11.7 ± 0.2
SiO ₂ (10 nm)	850	583 ± 3	30.1 ± 0.4	0.69 ± 0.01	12.1 ± 0.2
Current symmetry factor - CSF					
Without SiO ₂	840		0.16 ± 0.01		
SiO ₂ (10 nm)	850		0.14 ± 0.05		

on the front face. The CSF was very low for uncovered and SiO_2 covered solar cells. Thus, the rear passivation was not effective and/or the minority carrier lifetime was very low, resulting in the minority carrier diffusion length smaller than the wafer thickness. The Figure 2 shows the two-dimensional distribution of the minority charge carrier diffusion length in passivated and unpassivated devices. The bifacial solar cells without SiO_2 layer presented an average diffusion length of 70 μm . In oxide-passivated devices, the average L_D was of around 90 μm , also lower than the wafer thickness.

Table 2 summarizes the electrical characteristics of the best solar cells produced with local BSF. In order to assess the values of minority carrier lifetimes, front surface recombination velocity (S_f), rear surface recombination velocity (S_r) and specific series resistance (r_s), the bifacial cells were simulated by using the PC1D computer program²⁶ and these parameters were adjusted to fit in well the simulated V_{oc} , J_{sc} , FF and η to the experimental ones. Bearing in mind that Al-BSF covers 9.5% of the rear surface, an effective surface recombination velocity ($S_{r\text{-ef}}$)

was considered by using the method presented by Lago-Aurrekoetxea²⁷. The surface recombination velocity was set in 1×10^7 cm/s for the surfaces not covered by Al or SiO_2 . The following parameters were set to obtain the results presented in Table 2 for the cells without oxide: $S_f = 1 \times 10^7$ cm/s, $S_{r\text{-ef}} = 9.05 \times 10^6$ cm/s, $\tau = 10$ μs and $r_s = 2.8$ $\Omega \cdot \text{cm}^2$. When the cells were passivated with the thermally-grown SiO_2 layer, the parameters used in the simulations that led to the best I-V (electric current-voltage) curve fitting were: $S_f = 1 \times 10^5$ cm/s, $S_{r\text{-ef}} = 2.5 \times 10^4$ cm/s, $\tau = 10$ μs and $r_s = 2.8$ $\Omega \cdot \text{cm}^2$. Minority carrier lifetime was very low and high phosphorus doped emitter normally presents a high recombination velocity of around 10^5 cm/s, even if surfaces are SiO_2 coated. The combination of low minority carrier lifetime and high surface recombination led to the low current symmetry factor of these bifacial cells.

In order to evaluate the contamination and gettering mechanisms during the process, minority carrier lifetime (or bulk lifetime) was measured after each processing step and the results are shown in the Figure 3 and Figure 4. Oxides and emitter were etched away with an HF solution and the

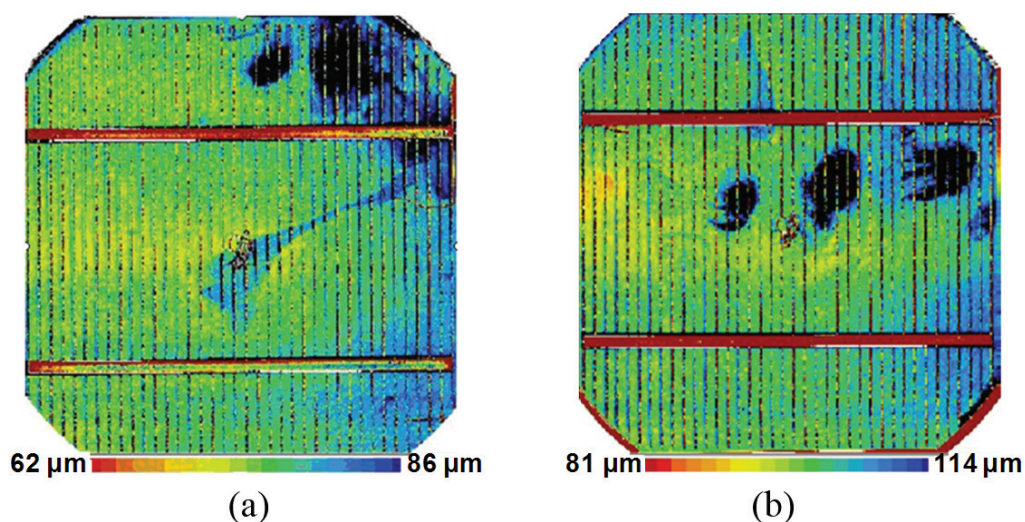


Figure 2. Two-dimensional distribution of the minority carrier diffusion length of the solar cells with local Al-doped BSF: (a) without SiO_2 layer (scale from 62 μm to 86 μm) and (b) with SiO_2 (81 μm to 114 μm).

Table 2. Electrical characteristics of the best bifacial solar cells with Al locally diffused BSF and results from simulation by means of the PC1D device-modeling program.

Front illumination (on n ⁺ p junction)						
	T_{Firing} ($^{\circ}\text{C}$)	Results	V_{oc} (mV)	J_{sc} (mA/cm^2)	FF	η (%)
Without SiO_2	840	Exp*	573	29.3	0.709	11.9
		Sim•	579	29.2	0.698	11.8
SiO_2 (10 nm)	850	Exp	585	30.5	0.688	12.3
		Sim	584	31.0	0.694	12.5
Current symmetry factor – CSF						
Without SiO_2	840	Exp	0.16			
		Sim	0.10			
SiO_2 (10 nm)	850	Exp	0.14			
		Sim	0.13			

*Experimental results; •Simulated results.

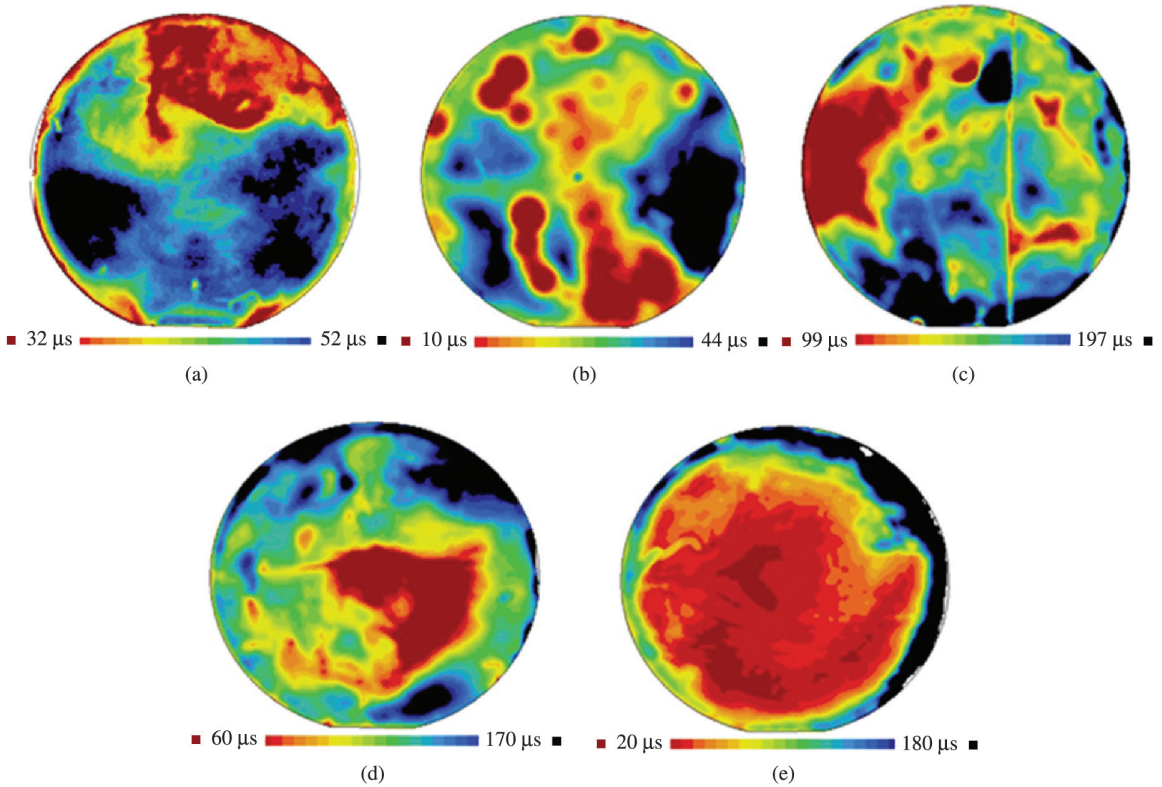


Figure 3. Minority charge carrier lifetime distribution after: (a) texture etching (32 μs to 52 μs), (b) oxide growth (10 μs to 44 μs), (c) P diffusion (99 μs to 197 μs), (d) passivation oxide growth (60 μs to 170 μs) and (e) metallization (20 μs to 180 μs).

CP4 one ($\text{HNO}_3:\text{HF}:\text{CH}_3\text{COOH}$). During the measurements, samples were immersed in an iodine+ethanol solution to passivate the surfaces. The metallization comprises three thermal steps in belt furnace, two of them for drying of the metal pastes (from 150 $^\circ\text{C}$ to 300 $^\circ\text{C}$) and one step for firing these pastes (840-850 $^\circ\text{C}$). To analyze the effect of this fabrication step on bulk lifetime, wafers were thermally processed without the metal grid. The results showed that bulk lifetime was enhanced by P gettering and the metallization step degraded the minority carrier lifetime.

In the Table 3 are summarized the results obtained from n^+pp^+ cells with selective BSF formed by boron diffusion over the whole rear surface and by Al locally diffused. Comparing the cells with local Al-BSF (Table 1) to those with Al/B-BSF, we can observe that the current symmetry factor was increased from 0.14 to 0.73 for passivated devices and from 0.16 to 0.64 in unpassivated cells. Oxide layer did not improve the cell output parameters.

The electrical parameters of the best solar cells with selective Al/B-BSF are presented in Table 4. The most efficient device presented the efficiency of 13.7% under front illumination (pn junction) and 8.9% under rear illumination (BSF region). Results from similar devices with smaller area (24.7 cm^2) were reported by Recart²³, achieving front efficiency slightly higher, but with the busbars outside the active area. The rear efficiency was 1.9% (absolute) higher than the obtained in this work because ARC was used.

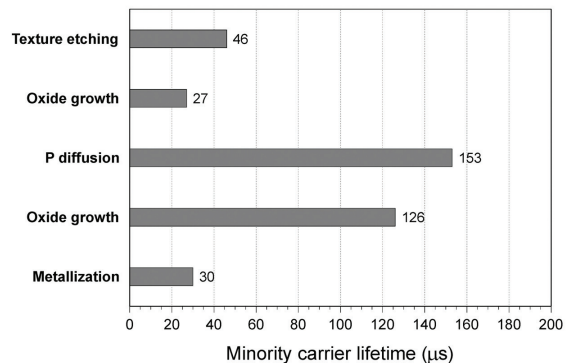


Figure 4. Average minority charge carrier lifetime after each processing step used to produce local-Al doped BSF.

Deposition of the ARC on the rear face can enhance the J_{sc} of around 2 mA/cm^2 and the efficiency can be improved to 10%.

The PC1D computer program was used for modeling these cells and the internal parameters such as τ , S_p , S_r and r_s were adjusted to fit simulation results to the experimental ones. For passivated cells, input parameters set to simulate the cell performance were: $S_f = 7 \times 10^5 \text{ cm/s}$, $S_r = 7 \times 10^5 \text{ cm/s}$, $\tau = 10 \mu\text{s}$ and $r_s = 3.4 \Omega \cdot \text{cm}^2$. To model the devices with non-passivated surfaces, parameters used were: $S_f = 1 \times 10^7 \text{ cm/s}$,

$S_r = 1 \times 10^7$ cm/s, $\tau = 20$ μ s and $r_s = 2$ Ω .cm². The thin SiO₂ layer did not produce an effective surface passivation for cells with Al/B-BSF. Likewise the solar cells with local-Al BSF, the bulk lifetime, between 10 μ s to 20 μ s, used to simulate the solar cell with selective BSF, was also very low. The average L_D obtained from LBIC measurements

reached values as high as 460 μ m (devices without SiO₂) and 500 μ m (oxide-passivated cells), as shown in Figure 5. The high L_D was not due to the high bulk lifetime, but due to the boron BSF that reduced the recombination rate on the rear face and it was considered in the estimation of L_D from LBIC measurements.

Table 3. Average electrical characteristics of bifacial solar cells with Al/B - BSF.

Front illumination (on n ⁺ p junction)					
	T_{Firing} (°C)	V_{oc} (mV)	J_{sc} (mA/cm ²)	FF	η (%)
Without SiO ₂	840	595 ± 2	31 ± 1	0.73 ± 0.01	13 ± 1
SiO ₂ (10 nm)	850	577 ± 13	29.4 ± 0.6	0.70 ± 0.01	11.9 ± 0.3
Rear illumination (on selective BSF region)					
Without SiO ₂	840	587 ± 1	19.7 ± 0.9	0.74 ± 0.01	8.6 ± 0.5
CSF			0.64 ± 0.05		
SiO ₂ (10 nm)	850	585 ± 5	21.5 ± 1.3	0.72 ± 0.04	9.0 ± 0.1
CSF			0.73 ± 0.06		

Table 4. Experimental and simulated electrical parameters of the best bifacial solar cells with Al/B-doped BSF region. The antireflection coating was not deposited on the rear face.

Front illumination (on n ⁺ p junction)						
	T_{Firing} (°C)	Results	V_{oc} (mV)	J_{sc} (mA/cm ²)	FF	η (%)
Without SiO ₂	840	Exp*	597	31.2	0.736	13.7
		Sim•	597	31.5	0.733	13.8
SiO ₂ (10 nm)	850	Exp	587	29.8	0.693	12.1
		Sim	593	31.5	0.664	12.4
Rear illumination (on selective BSF region – no ARC)						
Without SiO ₂	840	Exp	588	20.3	0.748	8.9
		CSF		0.65		
		Sim	585	19.2	0.765	8.6
		CSF		0.61		
SiO ₂ (10 nm)	850	Exp	582	22.4	0.687	9.0
		CSF		0.75		
		Sim	578	17.6	0.727	7.4
		CSF		0.56		

*Experimental results; •Simulated results.

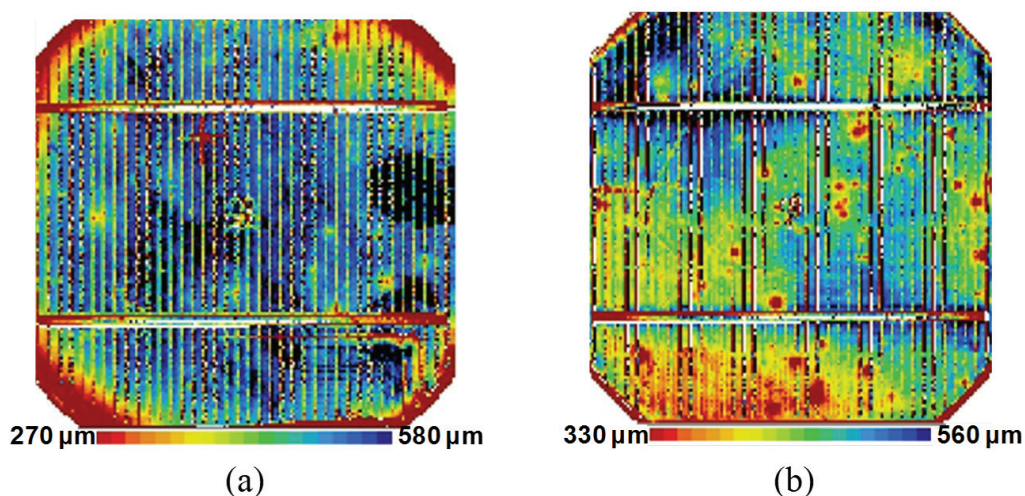


Figure 5. Two-dimensional distribution of the minority carrier diffusion length of the bifacial cells with boron/aluminum BSF: (a) unpassivated device (270 μ m to 580 μ m) and (b) SiO₂ – passivated solar cell (330 μ m to 560 μ m).

4. Conclusions

Local Al-doped BSF and selectively doped Al/B-BSF were implemented in thin bifacial silicon solar cells.

Concerning the solar cells with locally doped BSF, the analysis of the minority charge carrier lifetime showed that phosphorus diffusion produced gettering, but due to the contamination in belt furnace, bulk lifetime decreased and the final value was similar to the initial. Besides, the minority carrier diffusion length calculated from LBIC measurements was smaller than the wafer thickness. In addition, the silicon dioxide growth at 800 °C did not result in an effective surface passivation. The combined effect of low bulk lifetime and unpassivated rear surface led to the small CSF, lower than 0.16. Therefore, the structure was not suitable for bifacial devices.

The solar cells with a selective Al-B BSF presented higher current symmetry factors of around 0.70. Although the silicon dioxide layer established a poor rear surface passivation, the BSF in whole face allowed the achievement of average minority carrier diffusion lengths three times higher than the wafer thickness. The most efficient bifacial

cell was fabricated without SiO₂ layer and achieved an efficiency of 13.7% and 8.9% for front (n⁺ face) and rear (p⁺ face) illumination, respectively, the latter without ARC. The simulation of this cell with ARC on the rear face showed an improvement of around 2 mA/cm² in the J_{sc} and, consequently, the efficiency could rise to approximately 10%. The results obtained in this work were similar to that reported to bifacial devices with small area, but larger solar cells with spin-on boron deposition were developed and busbars were considered inside active area.

To sum up, thin bifacial solar cells need a selective BSF region when high quality surface passivation cannot be implemented in the industrial process.

Acknowledgements

The authors acknowledge the financial support provided by state utility CEEE-D (contract number CEEE-D 9942397) and by the Brazilian financing agencies FINEP (contract number 01.10.0020.02, ref. 2109/09) and CNPq (process number 563581/2010-7).

References

- Goodrich A, Hacke P, Wang Q, Sopori B, Margolis R, James TL, et al. A wafer-based monocrystalline silicon photovoltaics road map: utilizing known technology improvement opportunities for further reductions in manufacturing costs. *Solar Energy Materials and Solar Cells*. 2013; 114:110-135. <http://dx.doi.org/10.1016/j.solmat.2013.01.030>.
- Mauck M, Sims P, Rand J and Barnett A. Thin silicon solar cells. In: Markvart T, Castañer L, editors. *Solar cells: materials, manufacture and operation*. Oxford: Elsevier; 2005. p. 121-161. <http://dx.doi.org/10.1016/B978-185617457-2/50007-X>.
- Fischmann C, Giesen T, Böttinger F, Wertz R and Hoffmeister M. Automated handling and transport of crystalline photovoltaic wafers. In: *Proceedings of the 25th European Photovoltaic Solar Energy Conference and Exhibition*; 2010; Valencia, Spain. Valencia: WIP; 2010. p. 1677-1681.
- Hilali MM, Gee JM and Hacke P. Bow in screen-printed back-contact industrial silicon solar cells. *Solar Energy Materials and Solar Cells*. 2007; 91(13):1228-1233. <http://dx.doi.org/10.1016/j.solmat.2007.04.010>.
- Gu X, Yu X, Xu J, Fan R and Yang D. Towards thinner and low bowing silicon solar cells: form the boron and aluminum co-doped back surface field with thinner metallization film. *Progress in Photovoltaics: Research and Applications*. 2013; 21:456-461.
- Lee D-Y, Lee H-H, Yong Ahn J, Jung Park H, Kim JH, Kwon HJ, et al. A new back surface passivation stack for thin crystalline silicon solar cells with screen-printed back contacts. *Solar Energy Materials and Solar Cells*. 2011; 95(1):26-29. <http://dx.doi.org/10.1016/j.solmat.2010.05.004>.
- Cuevas A. The early history of bifacial solar cells. In: *Proceedings of the 20th European Photovoltaic Solar Energy Conference*; 2005; Barcelona, Spain. Barcelona: WIP; 2005. p. 801-805.
- Cuevas A, Luque A, Eguren J and del Alamo J. 50% more output power from an albedo-collecting flat panel using bifacial solar cells. *Solar Energy*. 1982; 29(5):419-420. [http://dx.doi.org/10.1016/0038-092X\(82\)90078-0](http://dx.doi.org/10.1016/0038-092X(82)90078-0).
- Moehlecke A and Krenzinger A. Modules assembled with diffuse reflectors for photovoltaic bifacial cells. In: *Proceedings of the 10th European Photovoltaic Solar Energy Conference*; 1991; Lisbon, Portugal. Lisbon: WIP; 1991. p. 967-970. http://dx.doi.org/10.1007/978-94-011-3622-8_247.
- Zanescio I and Lorenzo E. Optimisation of an asymmetric static concentrator: the PEC-44D. *Progress in Photovoltaics: Research and Applications*. 2002; 10(5):361-376. <http://dx.doi.org/10.1002/pip.431>.
- Norton B, Eames PC, Mallick TK, Huang MJ, McCormack SJ, Mondol JD, et al. Enhancing the performance of building integrated photovoltaics. *Solar Energy*. 2011; 85(8):1629-1664. <http://dx.doi.org/10.1016/j.solener.2009.10.004>.
- Coello J, Cañizo C and Luque A. Review on bifacial solar cell structures for industrialization. In: *Proceedings of the 21st European Photovoltaic Solar Energy Conference*; 2006; Dresden, Germany. Dresden: WIP; 2006. p. 1358-1361.
- Moehlecke A, Zanescio I, Cañizo C and Luque A. Experimental comparison between p and n bases for bifacial solar cells. In: *Proceedings of the 13th European Photovoltaic Solar Energy Conference*; 1995; Nice, France. Nice: WIP; 1995. p. 967-970.
- Jimeno JC, Bueno G, Lago R, Freire I, Pérez L, Recart F, et al. Low cost using ultra-thin bifacial cells. In: *Proceedings of the 22nd European Photovoltaic Solar Energy Conference*; 2007; Milan, Italy. Milan: WIP; 2007. p. 875-878.
- Yang L, Ye QH, Ebong A, Song WT, Zhang GJ, Wang JX, et al. High efficiency screen printed bifacial solar cells on monocrystalline Cz silicon. *Progress in Photovoltaics: Research and Applications*. 2011; 19(3):275-279. <http://dx.doi.org/10.1002/pip.1018>.
- Janßen L, Windgassen H, Bätzner DL, Bitnar B and Neuhaus H. Silicon nitride passivated bifacial Cz-silicon solar cells. *Solar Energy Materials and Solar Cells*. 2009; 93(8):1435-1439. <http://dx.doi.org/10.1016/j.solmat.2009.03.015>.
- Moehlecke A, Zanescio I and Luque A. Practical high efficiency bifacial solar cells. In: Conference Record of the IEEE First World Conference on Photovoltaic Energy Conversion; 1994; Hawaii, USA. Hawaii: IEEE; 1995. p. 1663-1666.

18. del Canizo C, Moehlecke A, Zanesco I, Tobias I and Luque A. Analysis of a technology for CZ bifacial solar cells. *IEEE Transactions on Electron Devices*. 2001; 48(10):2337-2341. <http://dx.doi.org/10.1109/16.954474>.
19. Buck I, Kopecek R, Libal J, Herguth A, Peter K, Rover I, et al. Industrial screen printed n-type silicon solar cells with front boron emitter and efficiencies exceeding 17%. In: *Proceedings of the 21st European Photovoltaic Solar Energy Conference*; 2006; Dresden, Germany. Dresden: WIP; 2006. p. 1264-1267.
20. Pan AC, Cañizo C and Luque A. Thin bifacial silicon solar cells. In: *Proceedings of the 22th European Photovoltaic Solar Energy Conference*; 2007; Milan, Italy. Milan: WIP; 2007. p. 1438-1441.
21. Pérez L, Coello J, Freire I, Varner K, Lago R, Bueno G, et al. Global processes for the fabrication of low cost bifacial solar cells. In: *Proceedings of the 20th European Photovoltaic Solar Energy Conference*; 2005; Barcelona, Spain. Barcelona: WIP; 2005. p. 891-894.
22. Recart F, Hoces I, Azkona N, Freire I, Pérez Manzano L, Fano V, et al. Bifacial thin solar cells with screen printed emitters and metallizations. In: *Proceedings of the 23rd European Photovoltaic Solar Energy Conference*; 2008; Valencia, Spain. Valencia: WIP; 2008. p. 1893-1896.
23. Recart F. *Evaluation of screen-printing as metallization technology for efficient solar cells*. [Doctor dissertation]. Spain: University of the Basque Country; 2001.
24. Steckemetz S, Metz A and Hezel R. Thin Cz-silicon solar cells with rear silicon nitride passivation and screen printed contacts. In: *Proceedings of the 17th European Photovoltaic Solar Energy Conference*; 2001; Munich, Germany. Munich: WIP; 2001. p. 1902-1906.
25. Conceição VC, Moehlecke A and Zanesco I. Analysis of the metal paste diffusion/firing process and the SiO₂ passivation in thin bifacial solar cells with p⁺ local region. In: *Proceedings of the IV Brazilian Solar Energy Congress and V ISES Latin American Conference*; 2012; São Paulo, Brazil. São Paulo: ABENS; 2012. p. 1-8. In Portuguese.
26. Basore PA and Clugston DA. PC1D version 5: 32-bit solar cell modeling on personal computers. In: *Proceedings of the 26th IEEE Photovoltaic Specialists Conference*; 1997; Anaheim, USA. Anaheim: IEEE; 1997. p. 207-210.
27. Lago-Aurrekoetxea R. *Surface and bulk recombination in silicon solar cells based on phosphorus-aluminum technology*. [Doctor dissertation]. Spain: Technical University of Madrid; 2002.